

CHAPTER 89

HYDRAULICS OF TIDAL INLETS ON SANDY COASTS

by

Ramiro Mayor-Mora, Dr. Eng.*

ABSTRACT

A series of laboratory experiments was carried out on an idealized ocean-inlet-bay system subjected to reversing flows caused by tidal and surface wave actions. The testing was done in a rectangular basin simulating a "bay" or "lagoon" and separated from an "ocean" basin by a sand barrier across which inlet pilot channels of varying cross sections and lengths were cut prior to starting each run; the ocean side of the barrier formed a 1:30 flat beach throughout the tests. Disturbances in the ocean were created by tide and wave generators. Their effects in the bay and inlet channel were measured by water level and current velocity recording units. Experimental measurements are presented here in normalized form in order to determine the relationships governing the hydraulic behaviour of a tidal inlet. These results are also compared to those obtained from a numerical approximation (the lumped parameter approach), all as functions of a proposed coefficient that includes the ocean-inlet-bay system characteristics. The experimental findings are further compared to available field data. Investigation of the effects of surface waves, controlling jetties, and fresh water inflow into the bay on the dimensionless parameters are also explored.

1. INTRODUCTION

Physical model studies are one of the alternatives to field data gathering in order to meet the need for understanding general processes occurring at and in the vicinity of tidal inlets on sandy coasts and for assessing the relative importance of the hydraulic parameters involved.

This paper summarizes major findings resulting from a laboratory investigation (1) carried out using a simplified model to reduce the complexity of the inlet, processes and their analysis. The model did not take account of inlet channel stability, sediment transport rates, salt water effects, flow patterns or littoral drift. The study included: the testing of movable-bed inlets with varying geometric characteristics, subjected to combinations of tides and surface waves whose effects are the generation of reversing flows that shape the inlet channels; the simultaneous measurement of the fluctuating water levels in the ocean, bay and inlet, and current velocities; the measurement of channel geometry at the end of each run; correlation of the parameters defining the hydraulic behaviour of the inlets; and comparison of the experimental results with those predicted by a numerical approximation and to some available field data.

* Senior Hydraulic and Coastal Engineering Specialist,
SNC INC. (Consultants), Montreal, Canada.

2. THE LUMPED PARAMETER APPROACH

The simplifications adopted to solve the simultaneous differential equations defining the hydraulics of a tidal inlet with fixed channel have decreased in number since Keulegan formulated his theoretical analysis (2). Huval and Wintergerst have included various important refinements to that analysis in a numerical solution known as "lumped parameter approach" (3) which accounts for non-sinusoidal ocean tide, variable bay surface area, variable inlet depth and cross sectional area throughout a tidal cycle due to sloping inlet banks and variable water levels, fresh water inflow into the bay and flow accelerations in the non-prismatic inlet channel.

The lumped parameter approach integrates the ordinary differential equations determining the water surface fluctuations:

$$h_o - h_b = \frac{1}{2g} \cdot (k_{en} + k_{ex} + \frac{fL}{4R}) \cdot |V| \cdot V + \frac{L}{g} \cdot \frac{\partial V}{\partial t} \quad \text{Eq. 1}$$

and

$$\frac{\partial h_b}{\partial t} = \frac{A \cdot V + Q_f}{AB} \quad \text{Eq. 2}$$

where, h_o and h_b are the water surface elevations in the ocean and in the bay respectively at time t , k_{en} and k_{ex} are the coefficients of energy losses due to channel entrance and exit, f the Darcy-Weisbach friction coefficient, L the length of the equivalent prismatic channel, R its hydraulic radius at time t , V the mean current velocity through A , the flow cross section, AB the bay surface area and Q_f the fresh water discharge into the bay. All parameters in Eq. 2 are functions of time.

In addition to a quadratic flow resistance assumption, Huval and Wintergerst assumed $k_{en} + k_{ex} = 1$ and f a function of Manning's coefficient.

For comparison to the experimental results, the computer program developed by Huval and Wintergerst was modified so that

$$k_{en} + k_{ex} + \frac{fL}{4R} = F \quad \text{Eq. 3}$$

where F , the inlet energy losses coefficient determined from measurements, became an input to the program as explained below.

3. TESTING PROGRAM AND DATA REDUCTION

A systematic series of 36 experimental runs was carried out on idealized ocean-inlet-bay systems involving reversing flows caused by tidal and uniform surface wave actions, at the Engineering Field Station of the University of California, Berkeley.

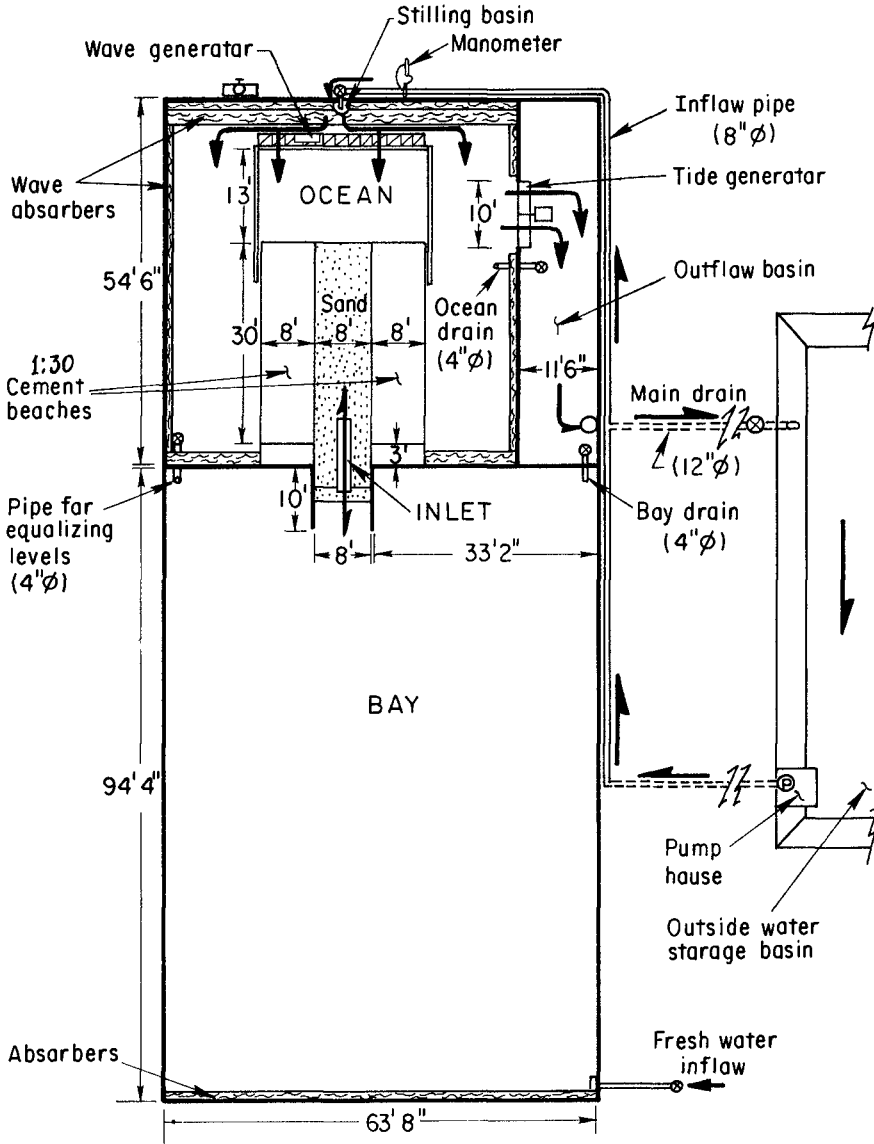


Fig. 1 - Schematic view of the testing facilities.

Fig. 1 illustrates the dimensions and components of the facilities. These were complemented by units continuously recording water level fluctuations, wave characteristics and current velocities, and devices for measuring and recording the inlet geometries. Fig. 2 shows the grain size characteristics of the sand used throughout the testing program to form a sloping barrier (1:30 on the ocean side) between the two basins.

Detailed descriptions of the facilities, equipment, instruments, testing procedures and resulting data have been reported elsewhere (1). Briefly, a typical run consisted in cutting a prismatic pilot channel through the sand barrier, activating the tide generator set at a tidal period of 20 to 60 minutes until a periodic bay tide motion was attained for several cycles at which time the run was terminated. The resulting inlet geometry was noted. A second part of the run was initiated by resuming the tidal action for a few cycles, followed by the introduction of uniform surface waves perpendicular to the initial inlet channel alignment as shown in Fig. 3. The photographs illustrate the behaviour of a short, deep inlet throughout a complete tidal cycle once periodic conditions were reached everywhere in the system. Inlet characteristics were again fully documented. Duration of each part of the run ranged from 4 to 25 hours.

Throughout the testing program, the following items were kept constant: surface area of the bay basin, beach slope, pilot channel bank slopes, and relative location of the walls defining the ocean basin, sand barrier and the bay.

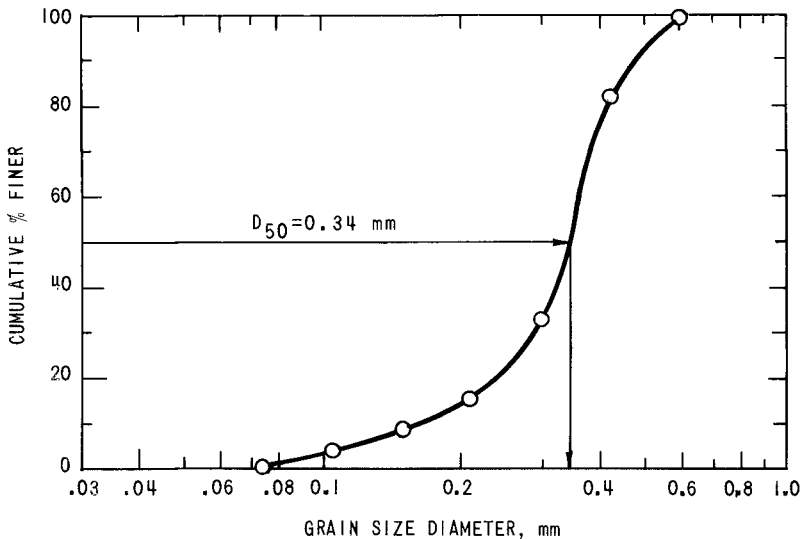


Fig. 2 - Sieve analysis of sand used in the testing.

Runs were also carried out to assess the effects of steeper surface waves (the rest of the runs with wave steepness under 0.024), parallel smooth-wall jetties (controlled condition) and fresh-water inflow into the bay (10.2 gpm).

Tide records were used for determining mean ocean and bay levels (MOL and MBL), ocean and bay ranges (RO and RB), time lags between ocean and bay high and low waters (EH and EL), duration of ebb and flood flows, as well as the slope of the bay tide curve at maximum discharge (dh_b/dt) and the ocean, inlet and bay water surface elevations (h_o , h_i and h_b , respectively) corresponding to that instant. Cross sectional areas (AMOL), surface widths (WMOL) and wetted perimeters (PMOL), were referred to the mean ocean level. In the case of runs with tidal action only, average values of the latter three parameters were computed whereas for runs with waves the throat region (vicinity of the cross section presenting the minimum flow area below MOL) was used for their computation. Clarification regarding all this parameters can be obtained by examining Fig. 4.

It has been shown (1) that repletion coefficients K, at maximum discharges ($dv/dt \approx 0$) can be obtained from measured parameters as follows:

$$K_f = \frac{T}{\pi \sqrt{2 RO} \cdot (h_o - h_b)_f} \cdot \frac{1}{\alpha_f} \cdot \left(\frac{\partial h_b}{\partial t} \right)_f^{\max} \quad \text{Eq. 4}$$

for flood flow, and

$$K_e = \frac{T}{\pi \sqrt{2 RO} \cdot (h_b - h_o)_e} \cdot \frac{1}{\alpha_e} \cdot \left(\frac{\partial h_b}{\partial t} \right)_e^{\max} \quad \text{Eq. 5}$$

for ebb flow, where T is the ocean tidal period and

$$\alpha = A/AMOL = 1 + [(WMOL + ETA \cdot h_i) \cdot h_i / AMOL] \quad \text{Eq. 6}$$

Accordingly, two values of K were computed for each inlet thus identifying the corresponding run. Using Keulegan's (1) definition of K, values of the inlet energy losses coefficient are obtained:

$$F_f = \left(\frac{\sqrt{g} \cdot T}{\pi \sqrt{RO}} \cdot \frac{AMOL}{AB} \cdot \frac{1}{K_f} \right)^2 \quad \text{Eq. 7}$$

for maximum flood discharge, and

$$F_e = \left(\frac{\sqrt{g} \cdot T}{\pi \sqrt{RO}} \cdot \frac{AMOL}{AB} \cdot \frac{1}{K_e} \right)^2 \quad \text{Eq. 8}$$

for maximum ebb discharge.

From equations 7 and 8 the expression

$$G = K_f \sqrt{F_f} = K_e \sqrt{F_e} = \frac{\sqrt{g} \cdot T}{\pi \sqrt{RO}} \cdot \frac{AMOL}{AB} \quad \text{Eq. 9}$$

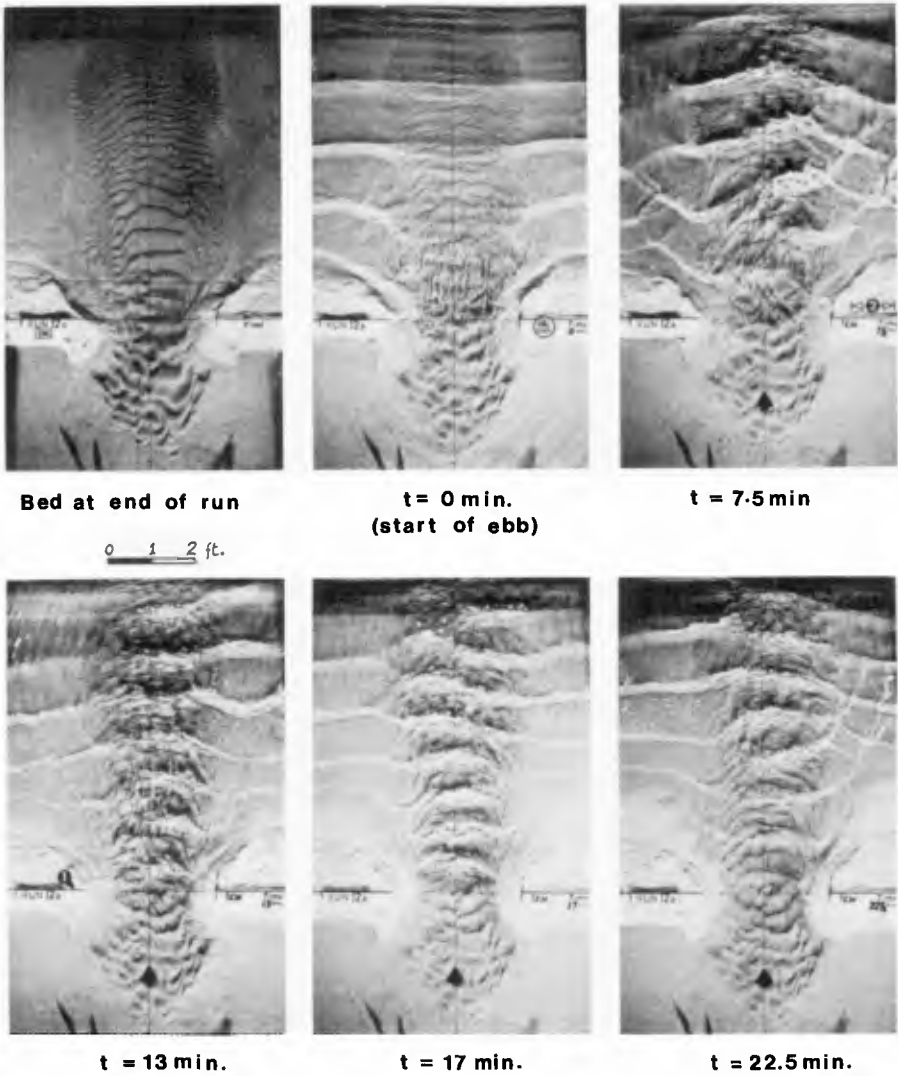


Fig. 3 - Model inlet under a 60-min. tidal cycle and 0.75-sec. uniform waves. EBBING.



**$t \approx 30$ min.
(start of flood)**



$t = 37.5$ min.



$t = 43$ min.



$t = 47$ min.

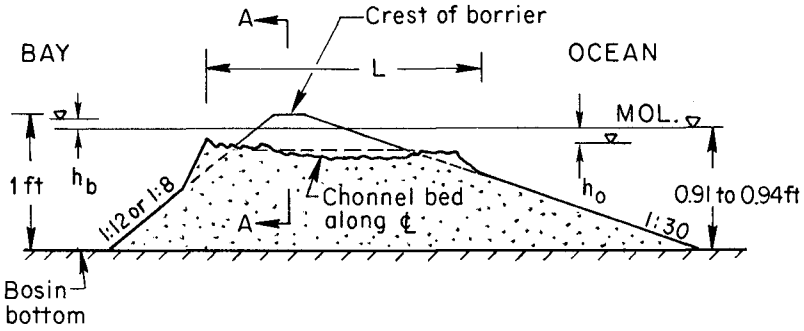


$t = 52.5$ min

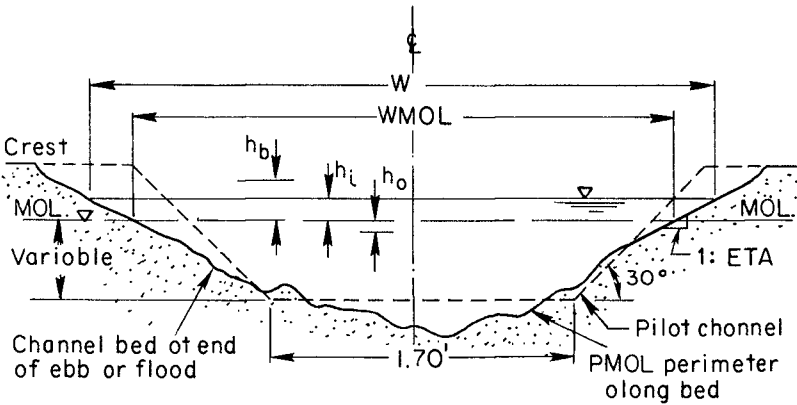


**$t = 60$ min.
(end of flood)**

Fig. 3 - (cont'd) Model inlet under a 60-min. tidal cycle and uniform waves. FLOODING.



b) Typical sand barrier profile along channel center line.



a) A-A Section: Typical flow cross section perpendicular to channel alignment.

Fig. 4- Longitudinal and transverse profiles of a typical sand barrier.

is obtained. G represents a dimensionless number, constant throughout a tidal cycle, defining the inlet characteristics and those of the ocean tide. G is a useful variable since its computation is based on quantities measurable both in the laboratory and in the field, making it unnecessary to estimate friction coefficients, exit and entrance energy loss coefficients or length of channel.

4. DIMENSIONLESS HYDRAULIC PARAMETERS VS. G .

Computations based on measurements yielded rough estimates of f at maximum discharges ranging from 0.01 to 0.65 but most of them from 0.05 to 0.20. Corresponding estimates of n ranged from 0.006 to 0.049, most of them within the 0.013 - 0.030 range.

For comparison to experimental results, data for each run were input to the lumped parameter program, the procedure for their treatment being: in the interest of time sinusoidal ocean tides were assumed with measured R_0 and T ; values of V and h_p were adopted as initial conditions, as well as time intervals and the approximate number of tidal cycles necessary for the results to show a periodic bay tide; values of n were then computed corresponding to maximum discharges for both ebb and flood flows. Two solutions were obtained (assuming that the roughness coefficients mentioned remain constant throughout the tidal cycle) but only that one corresponding to ebb flow roughness was retained for comparison because it showed closer agreement between actual measured parameters and results from the analytical solution; the reason for this probably being, among others, that a closer approximation to open channel flow (theoretical assumption) is evident during the ebb flow, the inlet behaving more like an orifice during flood. Computed values of n for ebb ranged from 0.016 to 0.049, most of them from 0.020 to 0.027.

Therefore, each run provided the absolute results as illustrated in Fig. 5 showing computer plots of ocean and bay tides, mean velocities and discharges during a cycle according to the lumped parameter approach compared to measured values of the first three variables. It should be pointed out that the measured velocity is a local one at the centre of the flow section, thus greater than the computed average. The case illustrated corresponds to a long and shallow inlet under tidal action, the analytical results based on an ebb flow value of n .

In addition to plots of absolute parameters, output included combinations of the results for all runs presented in dimensionless form thus allowing generalization of the findings as shown in the following figures, where the smooth curves are either best-fits or envelopes of the analytical results by the lumped parameter approach for uncontrolled inlets under either tidal action or simultaneous tidal and mild wave actions.

a. Ocean Tide Damping

The ratio of the bay and ocean tide ranges (Fig. 6) may be interpreted as a measure of the ability of an inlet to filter the ocean tide, where a high value indicates low damping efficiency. This ratio is very well predicted by the theory in the case of tidal action, and in a minor degree for the combined tidal and wave actions. Although not conclusive, it seems that

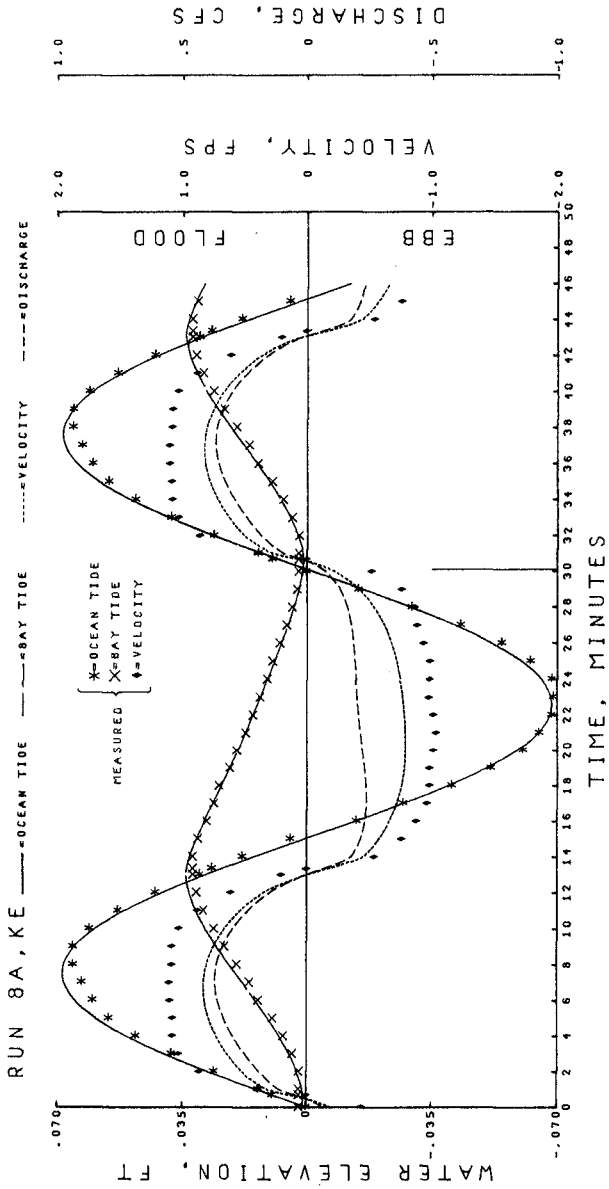
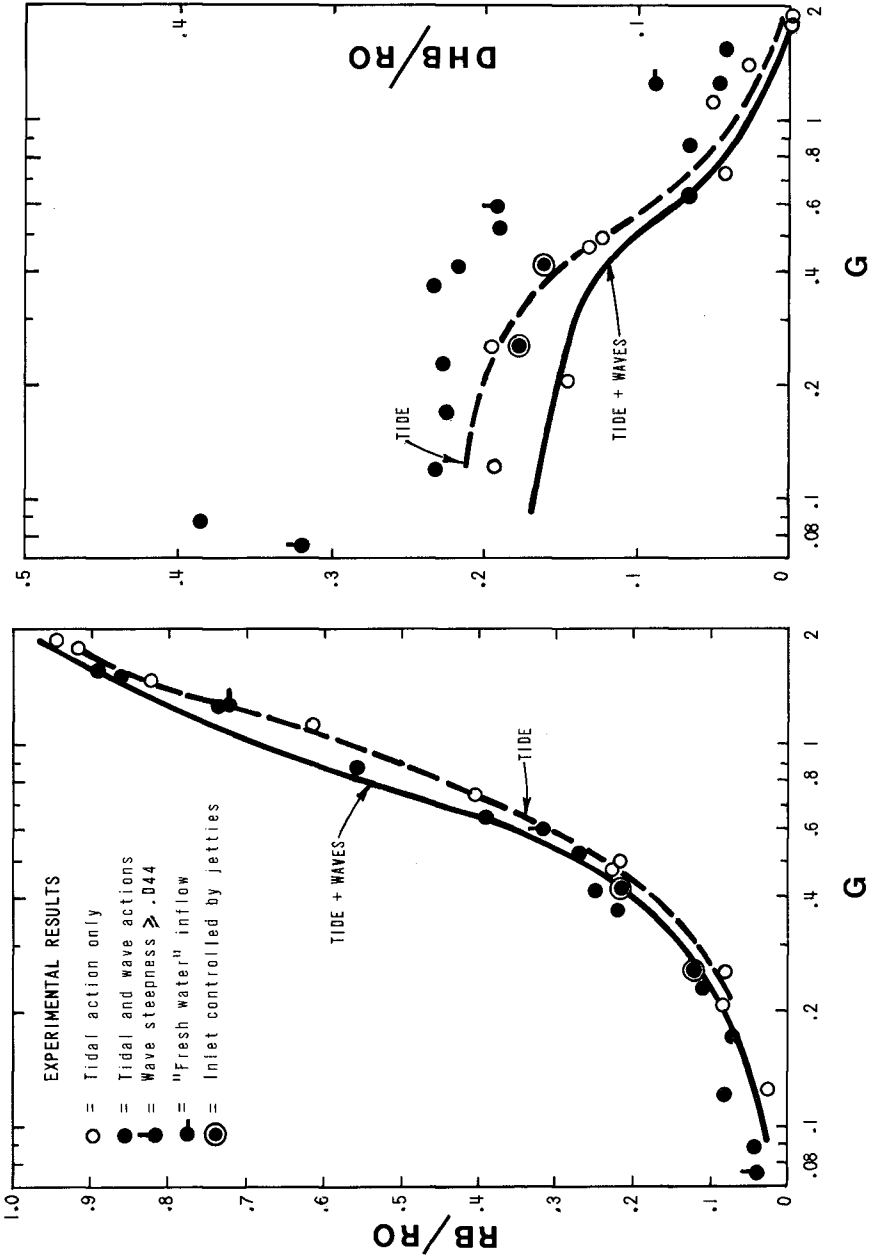


Fig. 5 - Comparison of measured parameters and theoretical solution by the lumped parameter approach, throughout a tidal cycle. $K = 0.179$.



a given inlet, steeper waves do not affect greatly the results obtained with milder waves. But the effect of waves on damping of the tide as compared to tidal inlets without much wave action is an increase in the tidal range of the bay, as predicted by the numerical approach and confirmed by the experiments. This effect appears to be reduced in the case of bays with fresh water inflows.

all damping ratios are found to be very sensitive to changes in the values of G (that is, changes in the bay and flow area characteristics for a given action) larger than 0.5, as evidenced by the steep sections of the curves.

Bay Superelevation

Fig. 6 also shows the difference between bay and ocean mean elevations (superelevation or DHB) divided by the ocean range and related to G . The superelevation predicted by the numerical method is longer under all action than under tidal and wave actions, specially for low G values, whereas experimental measurements indicate just the opposite, in addition to their large scatter. The mean bay waters are always above the ocean but the difference in the ratio decreases with increasing G . It is interesting to note that the inflexion points in the two sets of curves (tidal and wave action shown in Fig. 6 appear to occur at about the same value of G . Highest predicted values of superelevation are around 20% of tidal range whereas values close to 40% were measured. Keulegan's theory (2) did not predict bay superelevation.

Dimensionless Maximum Mean Current Velocity

maximum mean velocity across a flow section, V_{MAX} , can be approximated by

$$V_{MAX} = \frac{Q_{MAX}}{A_{MOL} \cdot \alpha} \quad \text{Eq. 10}$$

where Q_{MAX} is the maximum discharge through the inlet obtained by multiplying AB by the maximum slope of the recorded bay tide. Dimensionless values of maximum current velocities, AV_{MAX} , are expressed as

$$AV_{MAX} = \frac{Q_{MAX}}{\gamma \cdot AB \cdot RO/T} \quad \text{Eq. 11}$$

shown in Fig. 7 for both ocean conditions and for ebb and flood flows.

Most of the results based on experimental measurements are well predicted by the lumped parameter solution for inlets under tidal action only, the accuracy of the prediction being smaller in the case including waves. Theory shows that for a given inlet AV_{MAX} for flood is always higher than ebb value, fact that is confirmed by the experiments. However, it should be pointed out that this is not necessarily the case of absolute maximum mean velocities since the maximum velocity during ebb flow could be greater than that during flood.

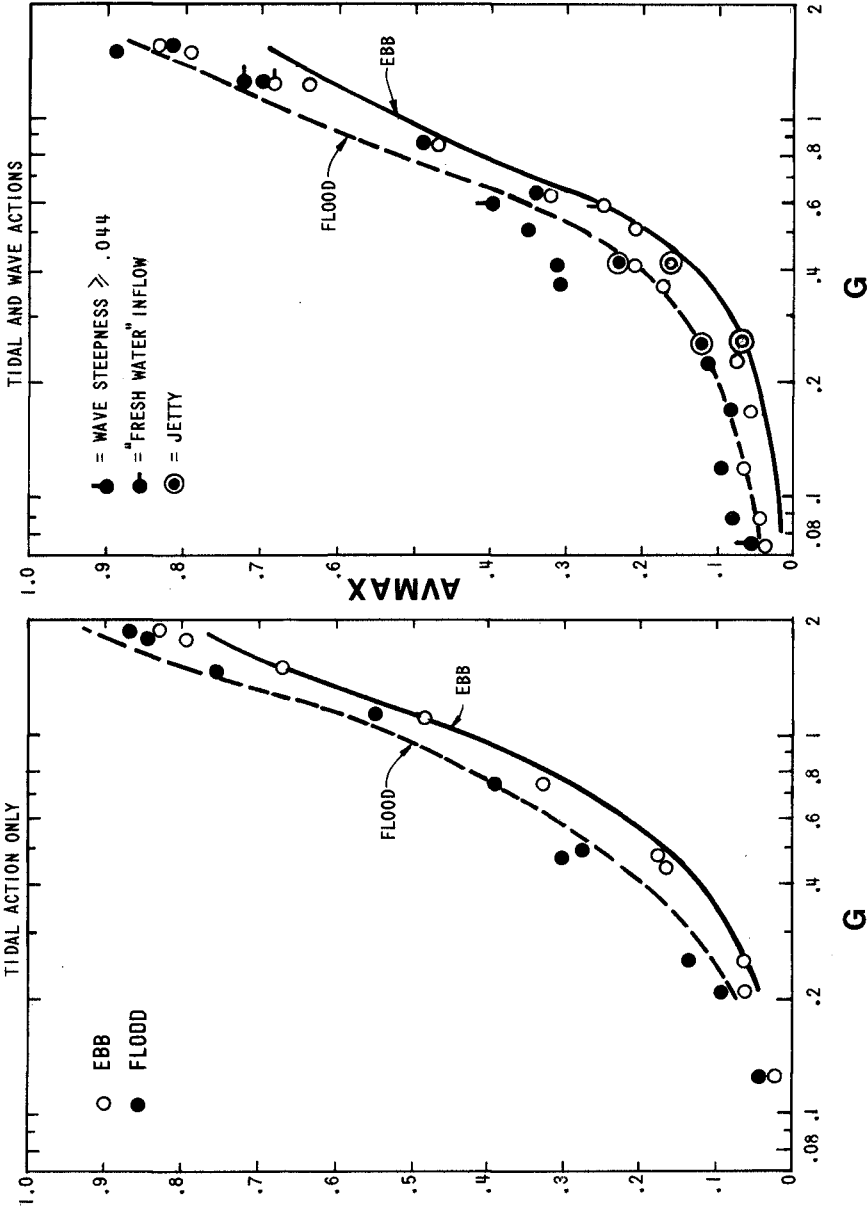


Fig. 7 - Dimensionless maximum mean current velocities as functions of the inlet G. Comparison of model measurements to the lumped parameter approach.

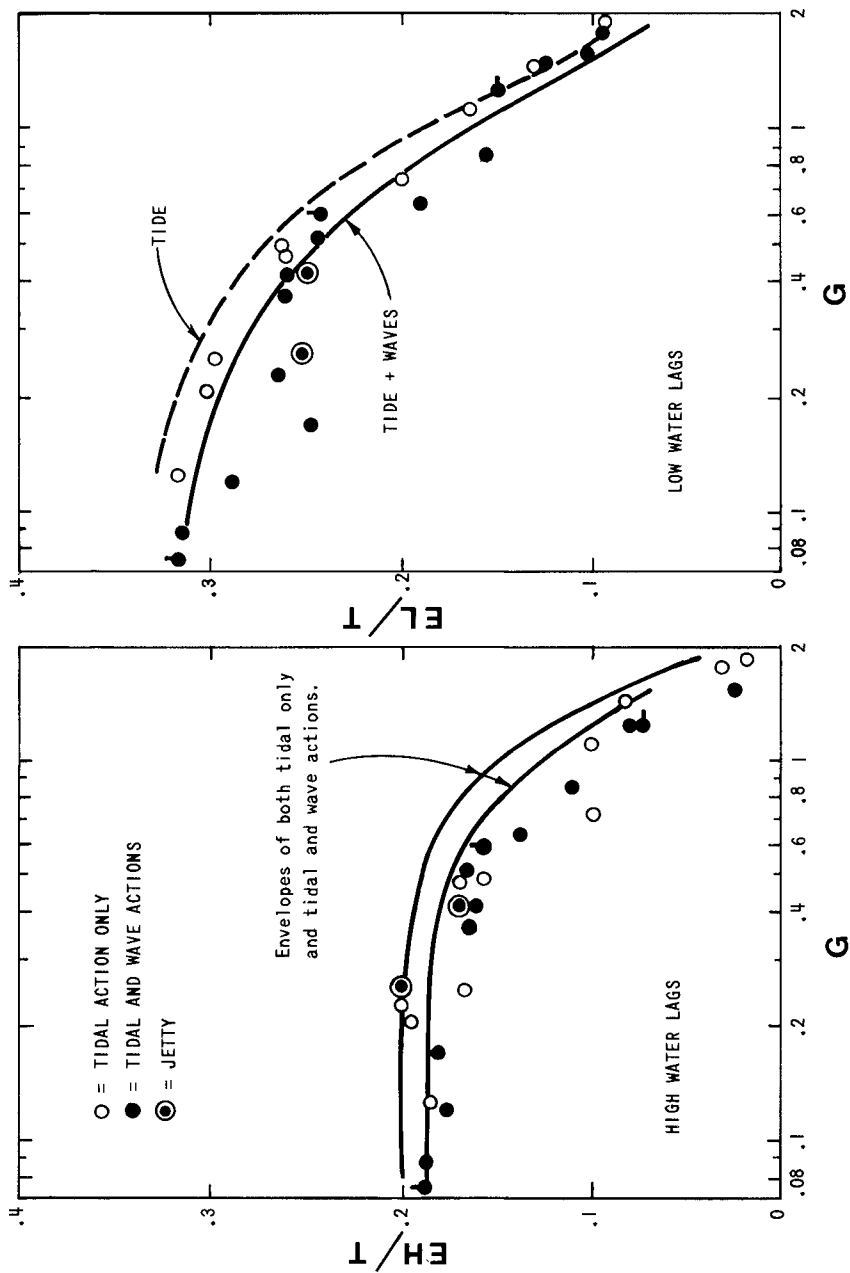


Fig. 8 - Dimensionless time lags between ocean and bay waters as functions of the inlet G . Comparison of model measurements to the lumped parameter approach.

d. Time Lags

The dimensionless time lags between ocean and bay high and low waters are shown as functions of G in Fig. 8. Lags between high waters are shorter than those between low waters in all types of inlets but the difference decreases as G increases. It could be said that, in general, the theory slightly overestimates the values of time lags. The high water lag results indicate that they reach an upper limit of close to 0.20 for G smaller than about 0.50, according to the lumped parameter approach. For high waters, the introduction of waves does not seem to affect the values of the lag, whereas it decreases somewhat the lag between low waters, as shown by both theoretical and experimental results. In other words, wave action accelerates the transmission of the ocean low water into the bay, specially in the case of inlets with low G values.

The above is visualized by the trends obtained from the tests and shown in Fig. 9: the dimensionless time lag between ocean and bay low waters (minima) is always longer than that corresponding to high waters (maxima). The 45° line in this figure corresponds to the basic Keulegan's development (2), the measurements for the tidal and wave action case being somewhat closer to such line.

e. Ebb and Flood Duration

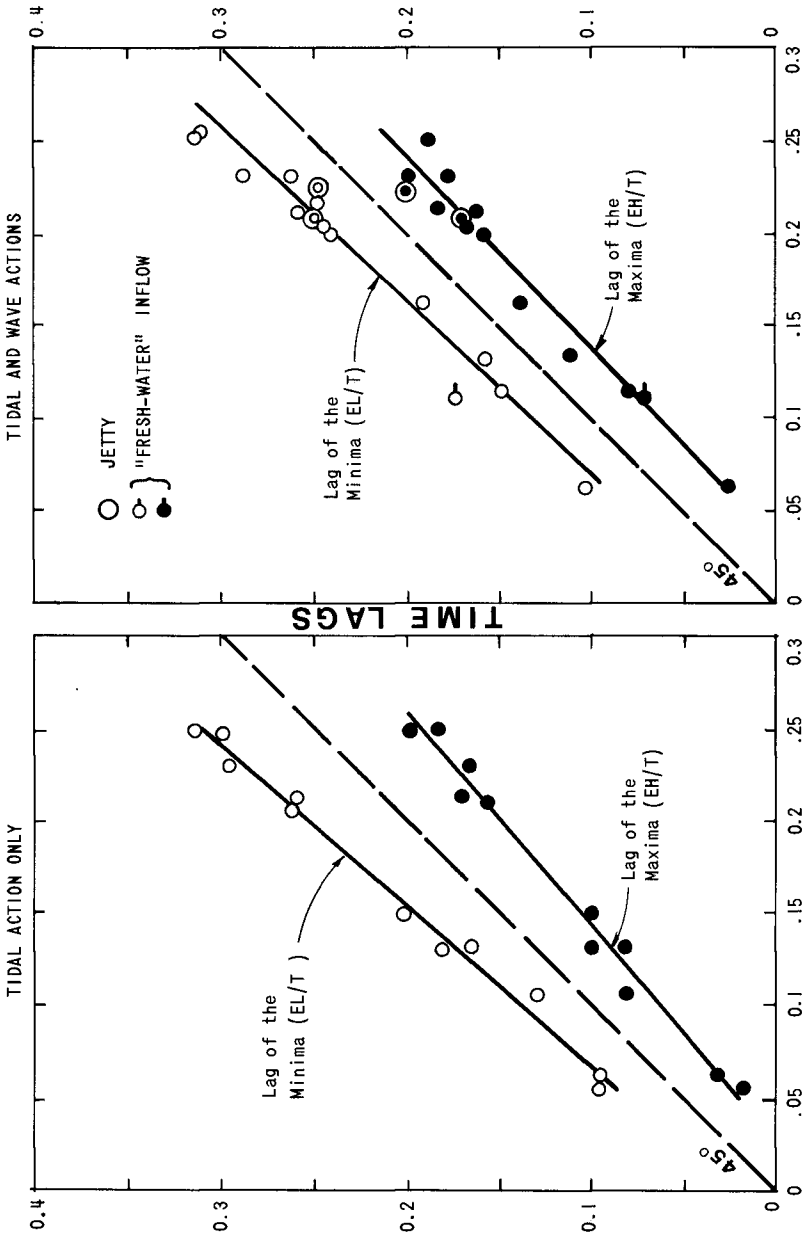
Fig. 10 shows the duration of both ebb and flood, i.e., the periods of time between slack waters at the inlet channel. In general, durations of ebb flow decrease with increases in G . These ebb durations are reduced when waves are introduced, up to values of G of about 0.50, whereas wave action does not seem to affect much the durations in the case of inlets with larger G coefficients. Keulegan's approximation (2) implied equal ebb and flow durations for any inlet.

f. Inlet Energy Loss Coefficient

F can be regarded as a measure of the resistance to flow presented by an inlet system at the instant of peak discharges in the channel. Experimental values of F (from Eqs. 7 and 8) are correlated with G as shown in Fig. 11, most of them being below 10. Inlets present a greater resistance to flow during the emptying of the bays than they do during the flood flow, the latter occurring at higher channel stages that diminish the effects from the rippled beds. These unit energy losses during the ebb flow are greater in the case of wave action specially for values of G smaller than about 0.60. On the other hand, unit losses during flood are not much affected by waves.

5. JETTIES, STEEP WAVES AND INFLOW INTO THE BAY

Regarding the exploratory tests, superelevations seem to decrease when controlling jetties are introduced but their influence on bay tidal range and dimensionless maximum mean velocities and lags is minor. Steeper waves cause somewhat higher bay superelevations and maximum mean velocities, but their effects on time lags are similar to those found for milder waves. As



AVG. TIME LAG

Fig. 9 - Dimensionless time lags compared to average time lags for a tidal cycle, and trends obtained from experimental measurements.

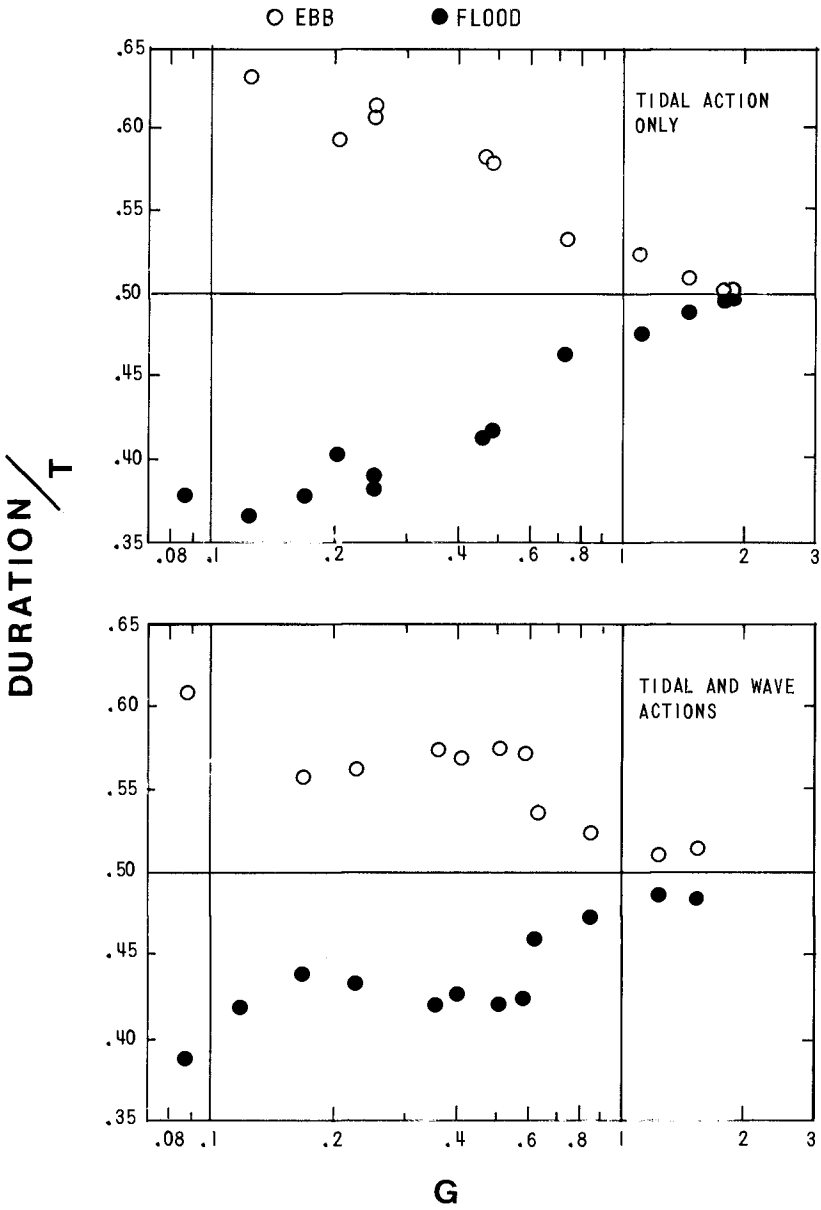


Fig. 10 - Dimensionless durations of ebb and flood as functions of the inlet G , obtained from experimental measurements.

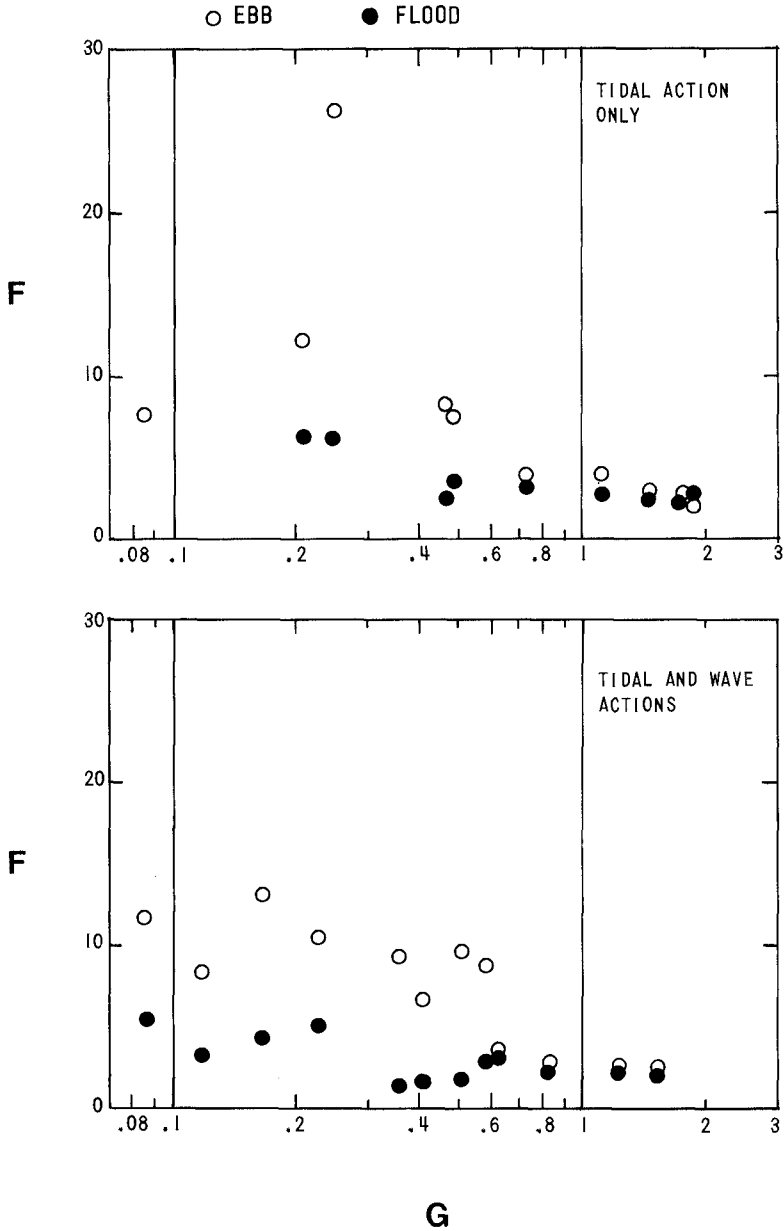


Fig. 11 - Inlet total loss coefficients (F) as functions of the inlet G, obtained from experimental measurements of uncontrolled inlets.

expected, fresh water inflow into the bay causes higher superelevations, lower values of dimensionless flood velocities and higher for those corresponding to ebb, whereas low water time lags are longer than those for similar bays with no fresh water inflows. Of course, more systematic research is needed for a complete assessment of all these effects.

6. TIDAL PRISM AND MINIMUM FLOW AREA

Since the requirement imposed by assuming that the water surface elevation was uniform throughout the bay was met in all runs (the ratio of the tidal wave length to the distance from the inlet to the bay furthestmost point varied from 65 to 200), for all practical purposes the bay water level moved up and down as a horizontal plane (1). The basin walls being vertical the experimental tidal prism P can be computed as

$$P = AB \cdot RB \quad \text{Eq. 12}$$

Tidal prisms on mean range for prototype inlets (1) and those for the model inlets are related to throat flow areas below MOL in Fig. 12. It is noted that the extension of the curve of experimental inlets with wave and tide action interacts prototype inlet conditions so model and field data seem to be governed by the same law regarding tidal prisms and minimum flow areas. However, the importance of the field data scatter is evidenced by the scale of relative differences shown in the figure. A further comparison is shown in Fig. 13 for unimproved inlets, including data from Nayak and Lin (1) for model inlets subjected to constant ebb flow only and field data for inlets without jetties and with one jetty not affecting the characteristics of the throat region.

7. CONCLUSION

With this simplified model it has been possible to further the knowledge of tidal inlet behaviour through the correlation of the various hydraulic parameters presented here as functions of the variable G . Most of the relationships are predicted by the lumped parameter approach with the exception of some of them related to combined tidal and wave actions. It should, however, be kept in mind that the numerical solution does not take into account wave effects. The relations between absolute tidal prisms and minimum inlet flow areas for both model and prototype were investigated, although the gap between field and laboratory measurements is still great.

The effects of controlling jetties, fresh water inflow into the bay and steep surface waves on the inlet hydraulics were explored. Much remains to be done in the investigations of these particular cases.

ACKNOWLEDGEMENTS

The study was supported by the following organizations: the University of California, Berkeley, the U.S. Army Corps of Engineers, the Quebec Ministry of Education and the consulting firm, Surveyer, Nenniger & Chênevert, Montreal, Canada

AMOL (sq. ft.)

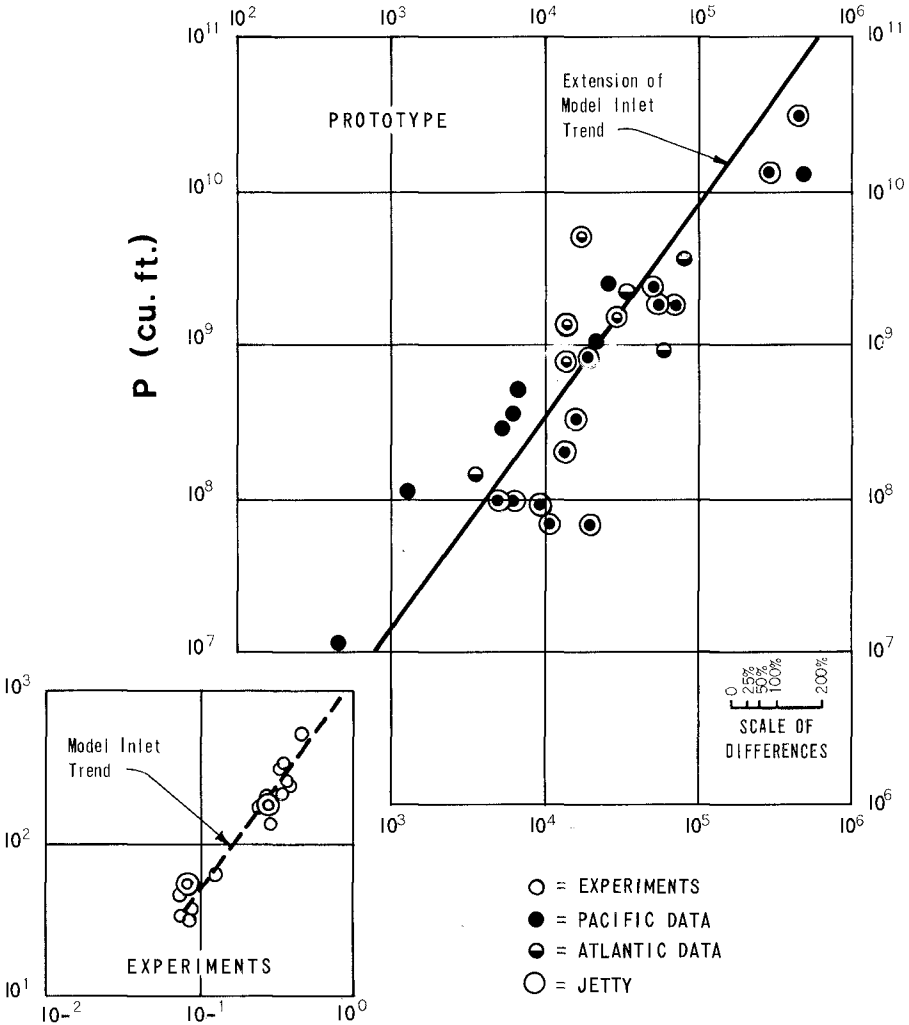
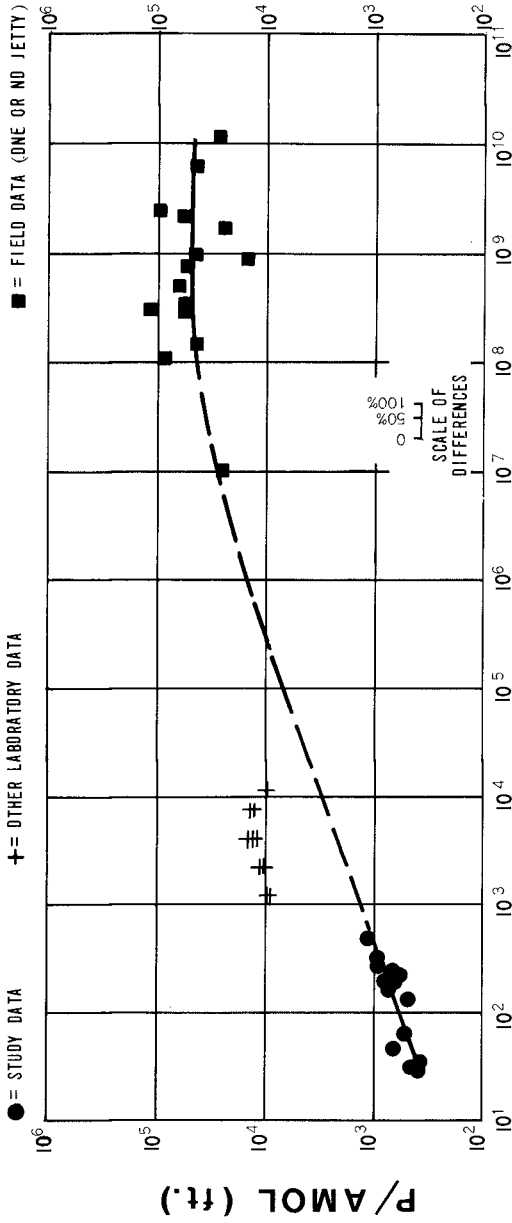


Fig. 12 - Relationship between minimum flow area and tidal prism (P) for some North American inlets and model inlets under tidal and wave actions.



P (cu. ft.)

Fig. 13 - Ratio of tidal prism (P) to minimum flow area as a function of the tidal prism. Comparison of laboratory and field data. Dashed line is a rough extrapolation of model and field trends.

REFERENCES

1. Mayor-Mora, R., "Hydraulics of Tidal Inlets on Sandy Coasts", University of California, Berkeley, Hydraulic Engineering Lab. Report HEL 24-16, August 1973.
2. Keulegan, G.H., "Tidal Flow in Entrances. Water Level Fluctuations of Basins in Communication with Seas," U.S. Army Corps of Engineers Tech. Bull. No. 14, of the Committee on Tidal Hydraulics, July 1967.
3. Huval, C.J., and Wintergerst, G.L., "Numerical Modeling of Tidal Inlet Hydraulics by the Lumped Parameter Approach", U.S. Army Corps of Engineers, Waterways Experiment Station, Vicksburg, Miss., January 1973 (Report draft).